Modeling the damage behavior of superplastic materials

H.S. da Costa-Mattos
Laboratory of Theoretical and Applied Mechanics, Department of Mechanical Engineering, Universidade Federal Fluminense, Niterói/RJ – Brazil
G. Minak, F. Di Gioacchino, A. Soldà
Department of Mechanical Engineering and Materials Science, University of Bologna, Bologna – Italy

Abstract

The present paper is concerned with the modeling of superplasticity phenomenon in metallic materials using a continuum damage theory. The goal is to propose a one-dimensional phenomenological damage model, as simple as possible, able to perform a mathematically correct and physically realistic description of plastic deformations, strain hardening, strain softening, strain rate sensitivity and damage (nucleation and growth of voids) observed in tensile tests performed at different strain rates. Only two tensile tests at different controlled strain rates are necessary to obtain all the material parameters that appear in the theory. Examples concerning the modeling of tensile tests of a magnesium alloy at different strain rates are presented and analyzed. The results obtained show a very good agreement between experimental results and model prevision.

Keywords: superplasticity, strain rate sensitivity, magnesium alloy, tension/compression testing, continuum damage mechanics.

1 Introduction

A wide class of materials – metals, ceramics, intermetalics, nanocrystaline, etc – show superplastic behavior under special processing conditions. Although, up to now, there is no precise physical definition of superplasticity phenomenon in metallic materials, from a phenomenological point of view, superplasticity can be defined as very high deformations prior to local failure. In the case of tensile tests under controlled strain rate, this means very high elongations of the specimens before rupture. The deformation process is generally conducted at high temperature and the strain can be 10 times the obtained under room temperature. Superplastically deformed material in tensile tests gets thinner in a very uniform manner, rather than forming a 'neck' (a local narrowing) which leads to fracture.

The most important characteristic of a superplastic material is its high strain rate sensitivity of flow stress that confers a high resistance to neck development and results in the high tensile elongations

Mechanics of Solids in Brazil 2009, H.S. da Costa Mattos & Marcílio Alves (Editors)
Brazilian Society of Mechanical Sciences and Engineering, ISBN 978-85-85769-43-7

characteristic of superplastic behavior. Superplasticity is used to form directly complex objects, by the application of gas pressure or with a tool, and often with the help of dies, avoiding complicated and costly joining and machine steps. The applications of superplastic formations were originally limited to the aerospace industry, but it has recently been expanded to include the automobile industries as a result of breakthroughs in the range of materials that can be made superplastic.

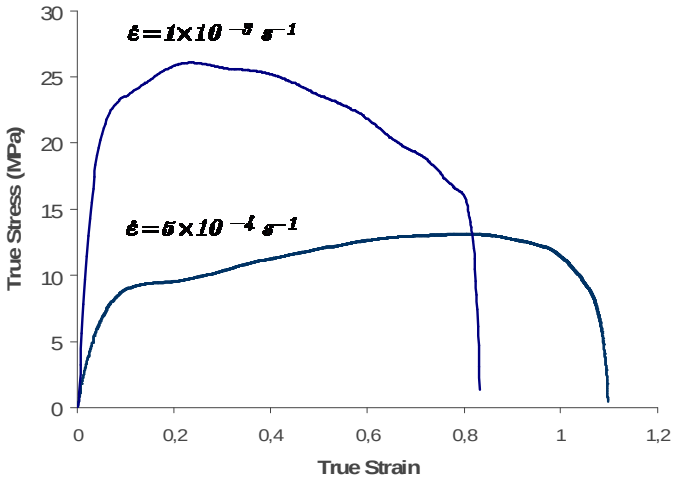

Figure 1: Strain hardening, strain softening, strain rate sensitivity and damage in AZ31B-F magnesium alloy at 400ºC.

The present paper is concerned with the modeling of such phenomenological behavior using a continuum damage theory. It is not the goal here to discuss the microscopic mechanisms of superplastic deformation. Most of the studies presented up to now in the literature are concerned with microstructural aspects of the phenomenon. In the case of superplasticity, the damage is mainly due to nucleation and growth of voids in the material. An interesting analysis of cavity initiation and growth can be found in Khaleel et al [1]. Other experimental works about superplastic behavior in magnesium alloys can be found in Kim et al [2]; Xin Wu and Yi Liu. [3]; Tan, [4]; Somekawa et al [5]; Lin et al [6]; Takuda et al [7]; Yin [8, 9]; Lee, et al [10].

2 Basic definitions

Let's consider a simple tension test in which the specimen has a gauge length L and cross section A_o submitted to a prescribed elongation $\Delta L(t)$. The force necessary to impose such elongation is noted $F(t)$.

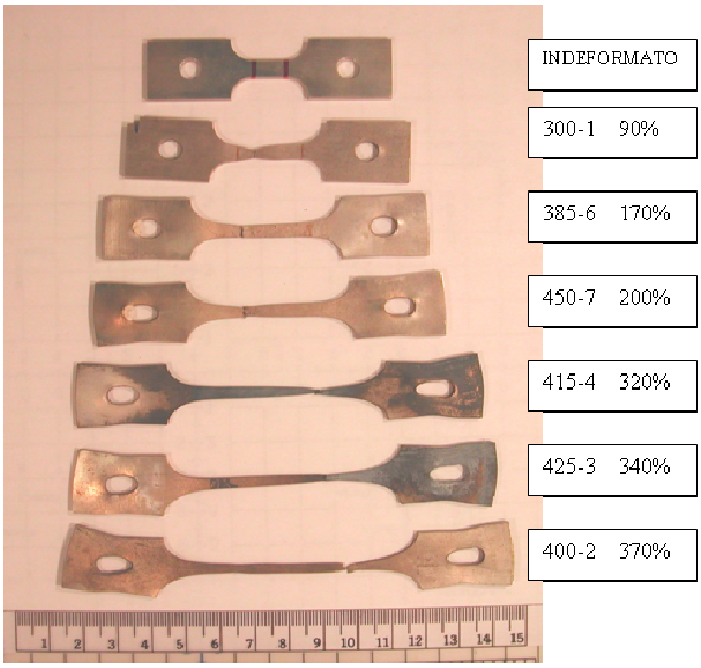

Figure 2: AZ31B-F magnesium alloy. Deformed specimens at different temperatures and strain rates.

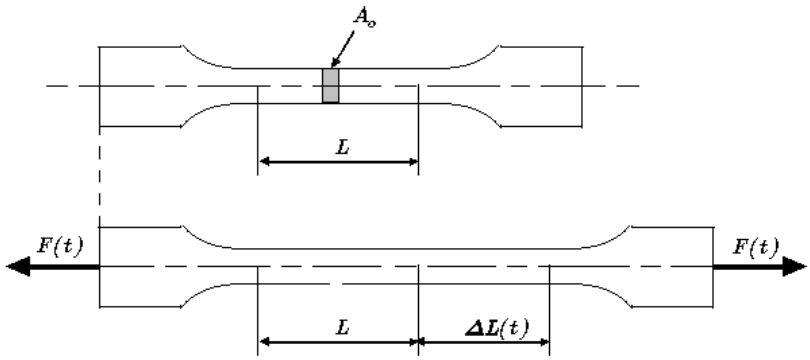

Figure 3: Specimen for a tensile test.

The so-called engineering strain ε and the engineering stress σ are defined as

$$\varepsilon(t) = \frac{\Delta L(t)}{L} \quad ; \quad \sigma(t) = \frac{F(t)}{A_o} \tag{1}$$

The so-called true strain ε_t and true stress σ_t are defined as

$$\varepsilon_t = \ln(1 + \varepsilon \quad ; \quad \sigma_t = \sigma(1 + \varepsilon) \tag{2}$$

From definitions (1) and (2) it is possible to obtain the following relations

$$\varepsilon_t = \ln(1 + \varepsilon) \;\Rightarrow\; \exp(\varepsilon_t) = \exp(\ln(1 + \varepsilon)) \;\Rightarrow \varepsilon = \exp(\varepsilon_t) - 1 \Rightarrow$$
$$\dot{\varepsilon} = \exp(\varepsilon_t)\dot{\varepsilon}_t \quad ; \quad \dot{\varepsilon}_t = \frac{\dot{\varepsilon}}{(1 + \varepsilon)} \tag{3}$$

The ASTM Standard E 2448-05 "Standard Test Method for Determining the Superplastic Properties of Metallic Sheet Materials" [11] describes the procedure for determining the superplastic forming properties (SPF) of a metallic sheet material. It includes tests both for the basic SPF properties and also for derived SPF properties. The test for basic properties encompasses effects due to strain hardening or softening.

3 Modeling the true stress against true strain curve without damage

The main idea of the model is to propose a very simple expression for the true stress σ_t *vs* true strain ε_t curve:

$$\textbf{HIP 1: } \sigma_t = a\ [1 - \exp(-b\varepsilon_t)]\,, \quad \text{with } a \text{ and } b \text{ being positive functions of } \varepsilon_t \text{ and } \dot{\varepsilon}_t \tag{4}$$

The dependency of the parameters a, b on ε_t and $\dot{\varepsilon}_t$ is the key to the definition of a physically realistic model. From experimental observations (see next section), it is possible to propose the following expression:

$$a(\varepsilon_t, \dot{\varepsilon}_t) \text{ is such that } \left[e^{(a-N_a)} - e^{(a_0-N_a)}\right] = \left[\dot{\varepsilon}_t \exp(\varepsilon_t)\right]^{K_a} \tag{5}$$

with a_o, K_a, N_a, being temperature dependent positive parameters. Since $\dot{\varepsilon} = \dot{\varepsilon}_t \exp(\varepsilon_t)$, a is constant in tensile tests with fixed value of the engineering strain rate $\dot{\varepsilon}$. Furthermore, it is easy to verify that $a = a_o$ when $\dot{\varepsilon} = 0$. From (5) it is possible to obtain the following relations:

$$\mathrm{e}^{\mathrm{a}}\mathrm{e}^{-\mathrm{N_a}} - \mathrm{e}^{\mathrm{a_o}}\mathrm{e}^{-\mathrm{N_a}} = \dot{\varepsilon}^{K_a} \Rightarrow$$
$$(\mathrm{e}^{\mathrm{a}} - \mathrm{e}^{\mathrm{a_o}})\,\mathrm{e}^{-\mathrm{N_a}} = \dot{\varepsilon}^{K_a} \Rightarrow$$
$$\ln(\mathrm{e}^{\mathrm{a}} - \mathrm{e}^{\mathrm{a_o}}) = K_a \ln(\dot{\varepsilon}) + N_a$$

If we define $\widehat{a} = \ln(\mathrm{e}^{\mathrm{a}} - \mathrm{e}^{\mathrm{a_o}})$, then

$$\mathrm{a} = \ln\left(e^{\widehat{a}} + \mathrm{e}^{\mathrm{a_o}}\right) \tag{6}$$

To simplify the model, it will be assumed from now on that $a_o = 0$, hence from (6):

$$a(\varepsilon_t, \dot{\varepsilon}_t) = \ln\left(e^{\widehat{a}} + 1\right) \quad \text{with} \quad \widehat{a} = K_a \ln(\dot{\varepsilon}) + N_a \tag{7}$$

The relation between coefficient a and the engineering strain rate $\dot{\varepsilon}$ is plotted below for the two different cases $a_o = 0$ and $a_o \neq 0$. It is evident that the obtained results differ only for lower strain rates.

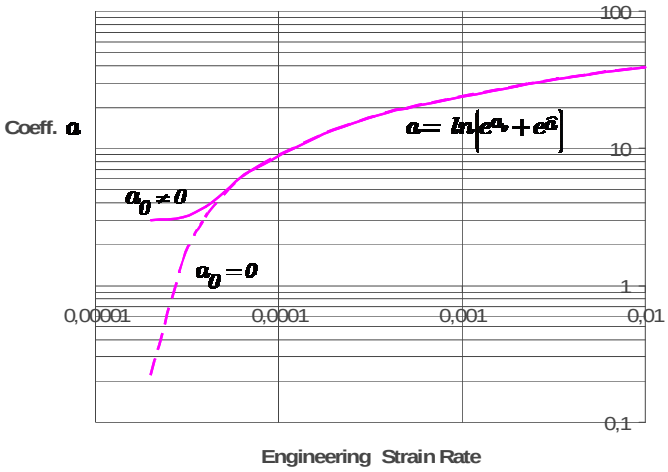

Figure 4: Variation of coefficient a with $a_0 = 0$ and $a_0 \neq 0$ for a magnesium alloy AZ31 at 375ºC.

Also from experimental observations, it is possible to propose:

$$b(\varepsilon_t, \dot{\varepsilon}_t) \text{ is such that } \left[e^{(ab - N_{ab})} - e^{(a_0 b_0 - N_a b)}\right] = \left[\dot{\varepsilon}_t \exp(\varepsilon_t)\right]^{K_{ab}} \tag{8}$$

with b_o, K_{ab}, N_{ab}, being temperature dependent positive parameters. Since $\dot{\varepsilon} = \dot{\varepsilon}_t \exp(\varepsilon_t)$, as shown for a, ab is constant in tensile tests with fixed value of the engineering strain rate $\dot{\varepsilon}$ and $ab = a_o b_o$ when $\dot{\varepsilon} = 0$. From (8) it is also possible to obtain the following relations:

$$\begin{aligned}
\mathrm{e^{ab}e^{-N_{ab}}} - \mathrm{e^{a_o b_o}e^{-N_{ab}}} &= \dot{\varepsilon}^{K_{ab}} \Rightarrow \\
\left(\mathrm{e^{ab}} - \mathrm{e^{a_o b_o}}\right)\mathrm{e^{-N_{ab}}} &= \dot{\varepsilon}^{K_{ab}} \Rightarrow \\
\ln\left(\mathrm{e^{ab}} - \mathrm{e^{a_o b_o}}\right) &= K_{ab}\ln(\dot{\varepsilon}) + N_{ab}
\end{aligned}$$

If we define $\widehat{ab} = \ln\left(\mathrm{e}^{\mathrm{ab}} - \mathrm{e}^{\mathrm{a_o b_o}}\right)$, then

$$ab = \ln\left(\mathrm{e} + \mathrm{e}^{\mathrm{a_o b_o}}\right) \quad \text{and} \quad \widehat{ab} = K_{ab}\ln\left(\dot{\varepsilon}\right) + N_{ab} \tag{9}$$

To simplify the model, it will be assumed from now on that $a_o b_o = 0$, hence:

$$ab(\varepsilon_t, \dot{\varepsilon}_t) = \ln\left(\mathrm{e}+1\right) \quad \text{with} \quad \widehat{ab} = K_{ab}\ln(\dot{\varepsilon}) + N_{ab} \tag{10}$$

Thus parameter $b(\varepsilon_t, \dot{\varepsilon}_t)$can now be expressed as ab and a ratio:

$$b(\varepsilon_t, \dot{\varepsilon}_t) = \frac{ab(\varepsilon_t, \dot{\varepsilon}_t)}{a(\varepsilon_t, \dot{\varepsilon}_t)} = \frac{\ln\left(\mathrm{e}+1\right)}{\ln\left(e^{\widehat{a}}+1\right)}$$

$$\text{with} \quad \widehat{a} = K_a\ln(\dot{\varepsilon}) + N_a \quad , \quad \widehat{ab} = K_{ab}\ln(\dot{\varepsilon}) + N_{ab} \tag{11}$$

Considering relation (3), it is easy to verify that b increases with increasing $\dot{\varepsilon}$ for $K_{ab} > K_a$ as shown in Fig.5 below

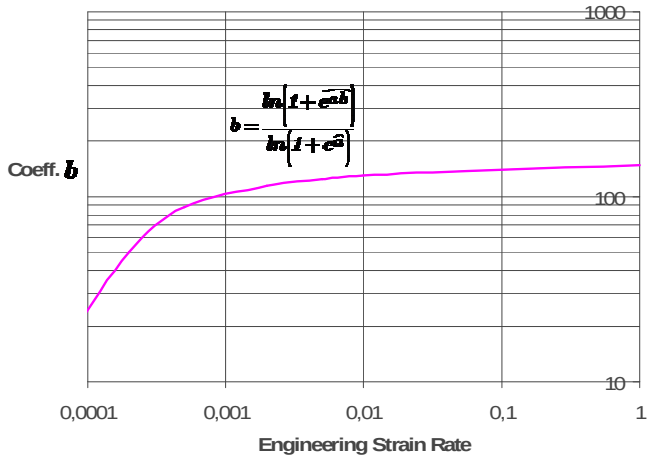

Figure 5: Variation of coefficient b for tensile tests at different strain rates ($K_{ab} > K_a$) for a magnesium alloy AZ31 at 375 ºC.

While b decreases with increasing $\dot{\varepsilon}$ for $K_{ab} < K_a$, Fig. 6.

Although expressions (5) and (8) are strongly non-linear, all parameters K_a, N_a, K_{ab}, N_{ab} can be identified from two tensile tests with constant engineering strain rates $\dot{\varepsilon}_1$ and $\dot{\varepsilon}_2$. In a tensile test with constant engineering stress rate $\dot{\varepsilon}_i$, from (4), true stress σ_t can be expressed as

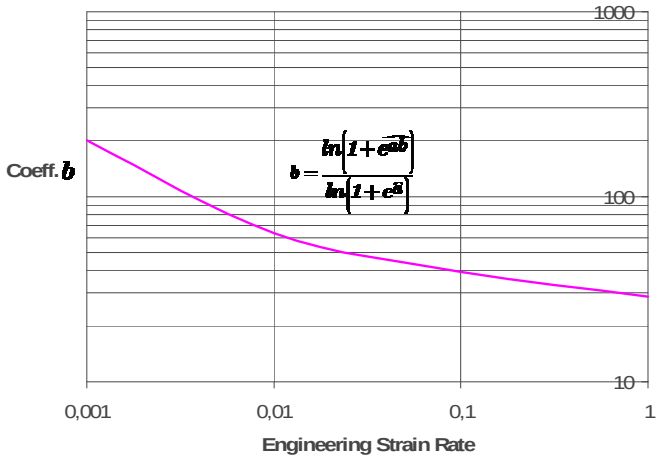

Figure 6: Variation of coefficient $b$for tensile tests at different strain rates ($K_{ab} < K_a$) for a magnesium alloy AZ31 at 500 °C.

$$\sigma_t = a_i \left[1 - \exp(-b_i \varepsilon_t)\right] \tag{12}$$

with

$$\widehat{a}_i = K_a \ln \left[\underbrace{\exp(\varepsilon_t)\ \dot{\varepsilon}_t}_{\dot{\varepsilon}_i} \right] + \mathrm{N}_a \tag{13a}$$

$$\widehat{a_i b_i} = K_{ab} \ln(\underbrace{\exp(\varepsilon_t)\ \dot{\varepsilon}_t}_{\dot{\varepsilon}_i}) + N_{ab} \tag{13b}$$

The parameters a_i and b_i can be identified from the true stress *vs* true strain curve obtained in a tensile test with constant engineering strain rate $\dot{\varepsilon}$ using a minimum squares curve fitting technique or using the following simpler procedure:

3.1 Identification of a_i

The parameter a_i can be identified from the true stress *vs* true strain curve. From (12), it is possible to obtain:

$$\lim_{\varepsilon_i \to \infty} (\sigma_t) = a_i \tag{14}$$

Hence, a_i is the maximum value of the stress σ_t.

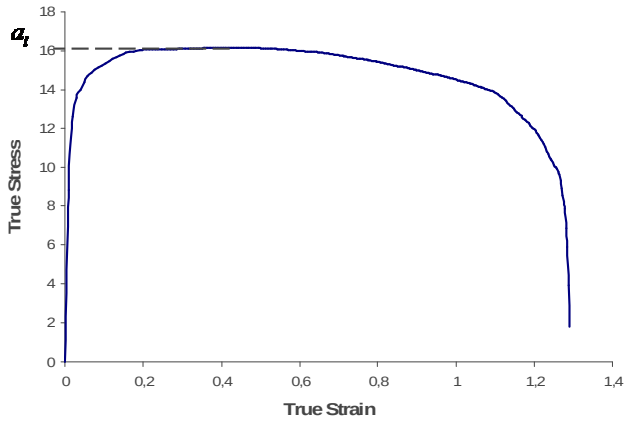

Figure 7: Identification of the parameter a_i from the true stress *vs* true strain curve.

3.2 Identification of b_i

From (12) it is also possible to verify that $\left.\frac{d\sigma_t}{d\varepsilon_t}\right|_{\varepsilon_t=0} = a_i b_i$

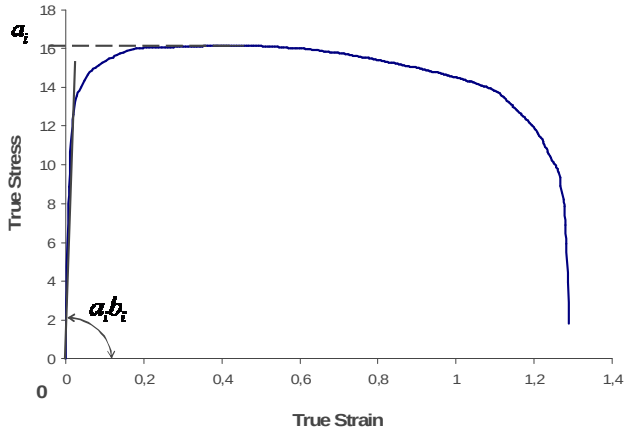

Figure 8: Identification of the parameter $a_i b_i$ from the true stress *vs* true strain curve.

Hence, once a_i is known, b_i can be identified from the initial slope of the true stress *vs* true strain curve. From (12) it is even possible to obtain

$$\exp(-b_i\varepsilon_t) = \left(\frac{a_i - \sigma_t}{a_i}\right) \quad \text{or,} \quad -b_i\varepsilon_t = \ln\left(\frac{a_i - \sigma_t}{a_i}\right)$$

Hence b_i can be approximated from the following expression:

$$b_i = -\left(\frac{1}{\varepsilon_t}\right)\ln\left(\frac{a_i - \sigma_t}{a_i}\right) \tag{15}$$

3.3 Identification of K_a, N_a, K_{ab}, N_{ab}

Once a_1, b_1 and a_2, b_2 are identified from two tensile tests with different engineering strain rates $\dot{\varepsilon}_1$ and $\dot{\varepsilon}_2$, the correspondent values of $\widehat{a}_1$, $\widehat{a}_2$ and $\widehat{a_1 b_1}$, $\widehat{a_2 b_2}$ are calculated from the definitions: $\widehat{a}_i = \ln\left(\mathrm{e}^{\mathrm{a_i}} - 1\right)$; $\widehat{a_i b_i} = \ln\left(\mathrm{e}^{\mathrm{a_i b_i}} - 1\right)$. These values permit to identified the parameters K_a, N_a, K_b, N_b as shown below.

From (13a) it is possible to obtain

$$\widehat{a_1} - K_a \ln(\dot{\varepsilon}_1) = N_a \tag{16}$$

and

$$-\left[\widehat{a_2} - K_a \ln(\dot{\varepsilon}_2) = N_a\right] \tag{17}$$

Hence, combining these equations it is possible to obtain

$$\widehat{a_1} - \widehat{a_2} = \mathrm{K_a}\left[\ln(\dot{\varepsilon}_1) - \ln(\dot{\varepsilon}_2)\right] \Rightarrow \mathrm{K_a} = \frac{\widehat{a_1} - \widehat{a_2}}{\ln(\dot{\varepsilon}_1) - \ln(\dot{\varepsilon}_2)} \tag{18}$$

The parameter K_a can be obtained from the following equation

$$N_a = -K_a \ln(\dot{\varepsilon}_1) \tag{19}$$

Once parameters K_a, N_a are known, it is possible to calculate $\widehat{a}_i$ for different strain rates and then obtain the correspondent a_i values from equation (7):

$$\mathrm{a_i} = \ln\left(1 + e^{\widehat{a_i}}\right) \tag{20}$$

With a similar procedure, from (13b), it is possible to verify that

$$\widehat{a_1 b_1} - K_{ab} \ln(\dot{\varepsilon}_1) = N_{ab} \tag{21}$$

and

$$-\left[\widehat{a_2 b_2} - K_{ab} \ln(\dot{\varepsilon}_2) = N_{ab}\right] \tag{22}$$

Hence, combining these equations it is possible to obtain

$$\widehat{a_1 b_1} - \widehat{a_2 b_2} = \mathrm{K_{ab}} \left[\ln\left(\dot{\varepsilon}_1\right) - \ln\left(\dot{\varepsilon}_2\right)\right] \Rightarrow \mathrm{K_{ab}} = \frac{\widehat{a_1 b_1} - \widehat{a_2 b_2}}{\ln\left(\dot{\varepsilon}_1\right) - \ln\left(\dot{\varepsilon}_2\right)} \tag{23}$$

Parameter N_{ab} can be obtained from the following equation

$$N_{ab} = -K_{ab} \ln\left(\dot{\varepsilon}_1\right) \tag{24}$$

Once parameters K_{ab}, N_{ab} are known, it is possible to calculate $\widehat{a_i b_i}$ for different strain rates and then obtain the correspondent $a_i b_i$ values from relation (10):

$$\mathrm{a_i b_i} = \ln\left(1 + e^{\widehat{a_i b_i}}\right) \tag{25}$$

Finally, it is possible to calculate b_i as $a_i b_i$ and a_i ratio.

$$b_i = \frac{a_i b_i}{a_i} \Rightarrow b_i = \frac{\ln\left(1 + e^{\widehat{a_i b_i}}\right)}{\ln\left(1 + e^{\widehat{a_i}}\right)} \tag{26}$$

3.4 Determination of material parameters for magnesium alloy AZ31 at 375°C with initial grain size d = 17μm

In this work, we examine the proposed constitutive equations for magnesium alloy AZ31 and identify the associated parameters. Magnesium alloys have recently attracted significant interest due to their excellent specific properties that make them potentially suitable candidates for replacing heavier materials in some automobile parts. Superplastic forming of Mg alloys is an alternative way of shaping these materials into complex geometries in one single operation. Thus, significant efforts are being lately devoted to understanding the underlying physical processes that take place during superplastic deformation of Mg alloys in order to improve their formability. The experimental results considered on this paper are taken from Del Valle et al. [12]. The Chemical Composition of an AZ31 magnesium alloy is presented on Table 1.

In order to identify the parameters that appear in the previous sections, two different series of experimental results referred to two tensile tests carried out at different strain rates ($\dot{\varepsilon}_1 = 0,0003$ (1/sec) and $\dot{\varepsilon}_2 = 0,01$ (1/sec)) have been considered.

For two different engineering strain rates $\dot{\varepsilon}_1 = 0,0003$ (1/sec) and $\dot{\varepsilon}_2 = 0,01$ (1/sec) we have

$$a_1 = 16,15 \text{ MPa} \; ; \; a_1 b_1 = 1130,5 \text{ MPa}; \; a_2 = 38,99 \text{ MPa} \; ; \; a_2 b_2 = 5068,7 \text{ MPa}.$$

From (18), (19), (23) and (24) it is possible to obtain

$$N_a = 0,251; \; K_a = 124,06 \; MPa; \; N_{ab} = 68.98; \; K_{ab} = 6,51 \; MPa$$

Table 1: Chemical Composition - Magnesium alloy AZ31.

Component	Value	Min	Max
Aluminum, Al		###	03:05
Calcium, Ca			00:04
Copper, Cu			00:05
Iron, Fe			0.005
Magnesium, Mg	97		
Manganese, Mn		###	
Nickel, Ni			0.005
Silicon, Si			00:01
Zinc, Zn		###	01:04

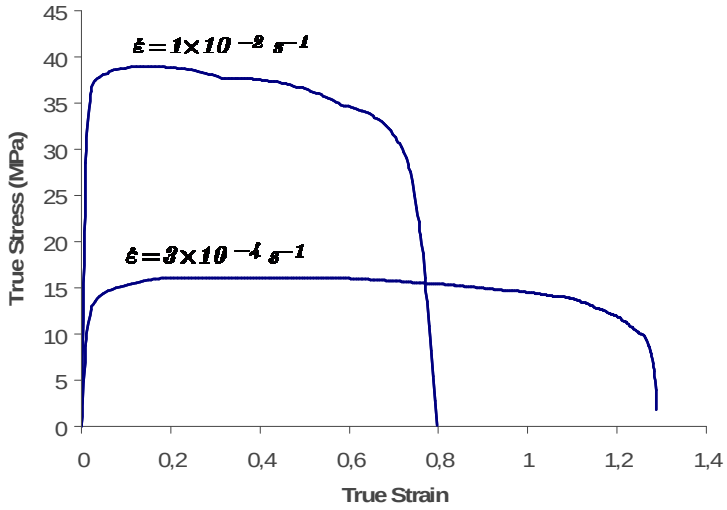

Figure 9: Magnesium alloy AZ31 at 375 ^{o}C. Two different strain rates $\dot{\varepsilon}_1 = 0,0003$ (1/sec) and $\dot{\varepsilon}_2 = 0,01$ (1/sec).

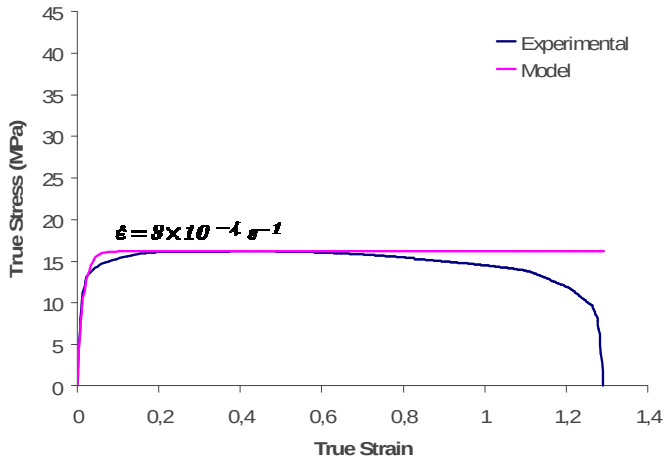

Figure 10: Stress-strain curve and model curve for $\dot{\varepsilon}_1 = 0,0003$ (1/sec).

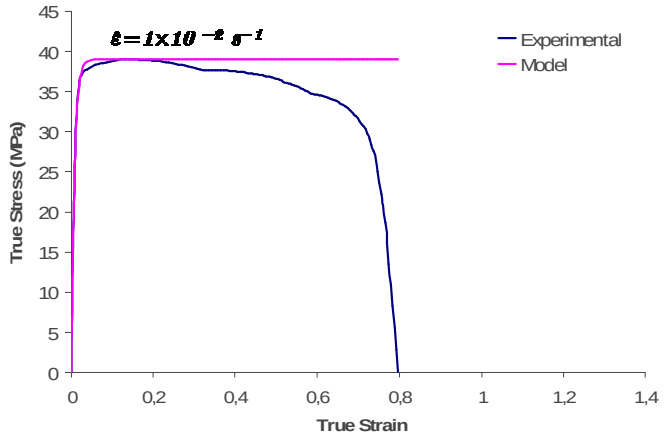

Figure 11: Stress-strain and model curve for $\dot{\varepsilon}_2 = 0,01$ (1/sec).

4 Modeling the true stress against true strain curve with damage

Only a few damage models were proposed for superplastic alloys, such as Chandra [13]. In the present paper it is introduced an auxiliary variable D that accounts for the nucleation and growth of voids observed in tensile tests performed at different strain rates.

$$\textbf{HIP 2: } \sigma_t = (1-D)\ a\ [1-\exp(-b\varepsilon_t)] \quad \text{with} \quad 0 \leqslant D \leqslant 1 \tag{27}$$

$$\textbf{HIP 3: } D = \begin{cases} 0, \text{ if } AUX > 1 \\ -\left[\dfrac{1}{b_d}\right] \ln(AUX), \text{ if } 0 < AUX < 1 \quad \text{with} \quad AUX = 1 - \left(\dfrac{\varepsilon_t - K_d/b}{a_d}\right) \\ 1, \text{ if } AUX < 0 \end{cases} \tag{28}$$

Where

$$a_d = -K_{a_d}(\dot{\varepsilon}) + N_{a_d}, \text{ and} \tag{29a}$$

$$\mathrm{a_d b_d} = K_{a_d b_d}[\dot{\varepsilon}]^{-N_{a_d b_d}} \tag{29b}$$

All parameters K_d, N_d, a_d, b_d can be identified from two tensile tests with constant engineering strain rates $\dot{\varepsilon}_1$ and $\dot{\varepsilon}_2$. Considering HIP 2. For a tensile test with constant stress rate $\dot{\varepsilon}_i$, the damage variable D can be expressed as $\frac{\sigma_t}{a[1-\exp(-b\varepsilon_t)]} = (1-D) \Rightarrow D = 1 - \frac{\sigma_t}{a[1-\exp(-b\varepsilon_t)]}$, after the softening behavior. Hence, the experimental curve D *vs* ε_t can be easily obtained.

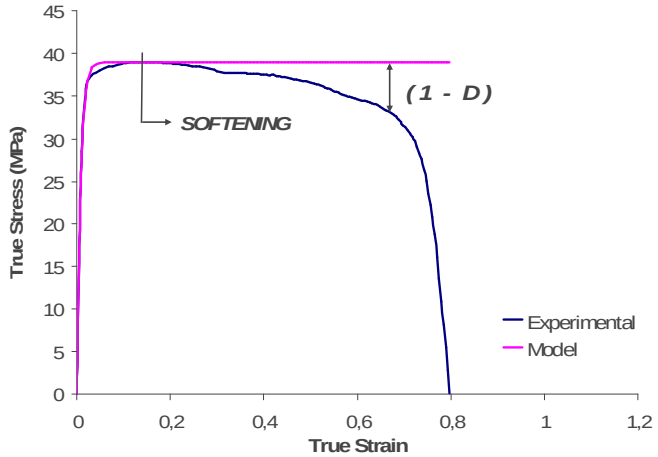

Figure 12: Experimental identification of the auxiliary variable D.

Since $\dot{\varepsilon} = \exp(\varepsilon_t)\dot{\varepsilon}_t$, it is possible to obtain from HIP 3

$$
\begin{aligned}
D = -\left[\frac{1}{b_d}\right] \ \ln\left[1 - \left(\frac{\varepsilon_t - \mathrm{K_d/b}}{a_d}\right)\right], \ \text{for } D \in [0,1) \Rightarrow \\
-b_d D = \ \ln\left[1 - \left(\frac{\varepsilon_t - \mathrm{K_d/b}}{a_d}\right)\right], \ \text{for } D \in [0,1) \Rightarrow \\
\exp(-b_d D) = \ 1 - \left(\frac{\varepsilon_t - \mathrm{K_d/b}}{a_d}\right), \ \text{for } D \in [0,1) \Rightarrow \\
\left(\frac{\varepsilon_t - \mathrm{K_d/b}}{a_d}\right) = \ 1 - \ \exp(-b_d D), \ \text{for } D \in [0,1) \Rightarrow \\
(\varepsilon_t - \mathrm{K_d/b}) = a_d\left[1 - \ \exp(-b_d D)\right], \ \text{for} D \in [0,1) \Rightarrow \\
\varepsilon_t \ = a_d\left[1 - \ \exp(-b_d D)\right] + \mathrm{K_d/b}
\end{aligned}
\tag{30}
$$

Parameters a_i and b_i can be identified from the true stress *vs* true strain curve obtained in a tensile test with constant engineering strain rate $\dot{\varepsilon}$ using a minimum squares curve fitting technique or using the following simpler procedure. If $D = 0$, from (22) it is possible to obtain

$$\varepsilon_t = \frac{\mathrm{K_d}}{\mathrm{b}}$$

A "corrected curve" is obtained by eliminating the viscous term $\mathrm{K_d/b}$ from this curve.

$$(\varepsilon_t)_{\text{corrected}} \ = a_d\left[1 - \ \exp(-b_d D)\right] \tag{31}$$

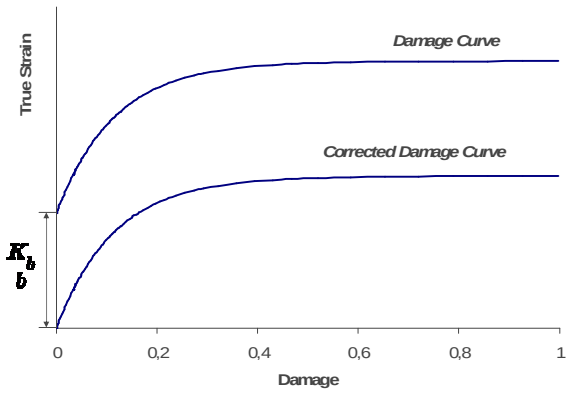

Figure 13: Damage curve and corrected damage curve obtained from a tensile test with constant engineering stress rate.

Parameters a_i and b_i can be identified from the true stress *vs* true strain curve using a minimum squares curve fitting technique or using the following simpler procedure.

4.1 Identification of a_d

From (31), it is possible to obtain:

$$\lim_{D\to 1}\left((\varepsilon_t)_{\text{corrected}}\right) = a_d \tag{32}$$

Hence, a_d is the value of the corrected strain $(\varepsilon_t)_{\text{corrected}}$ when $D \to 1$

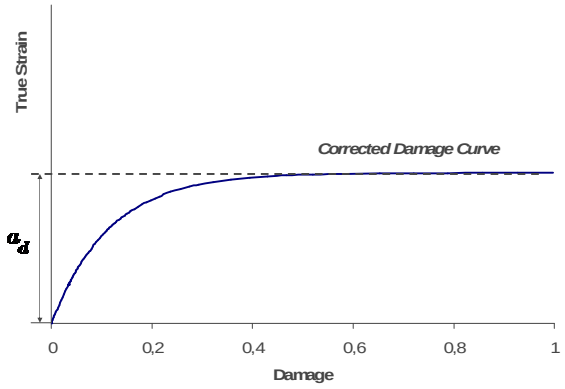

Figure 14: Experimental identification of a_d.

4.2 Identification of b_d

From (31) it is possible to verify that

$$\left.\frac{d(\varepsilon_t)_{\text{corrected}}}{dD}\right|_{D=0} = a_d b_d$$

Hence, once a_d is known, b_d can be identified from the initial slope of the true corrected damage curve. From (30) it is possible to obtain

$$\exp(-b_d D) = \left(\frac{a_d - (\varepsilon_t)_{\text{corrected}}}{a_d}\right) \quad \text{or,} \quad -b_d D = \ln\left(\frac{a_d - (\varepsilon_t)_{\text{corrected}}}{a_d}\right)$$

b_d can be approximated from the following expression:

$$b_d = -\left(\frac{1}{D}\right)\ln\left(\frac{a_d - (\varepsilon_t)_{\text{corrected}}}{a_d}\right) \tag{33}$$

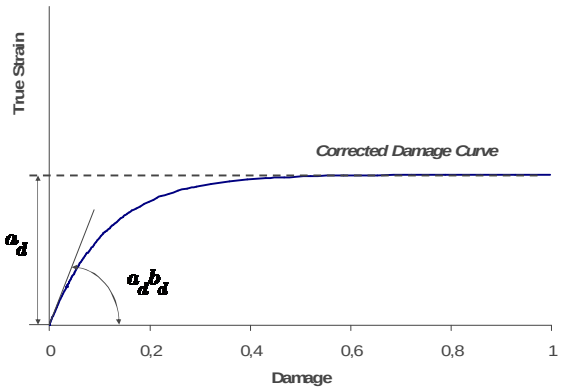

Figure 15: Identification of the parameter b_i from the true stress *vs* true strain curve.

4.3 Identification of K_{a_d}, N_{a_d}, $K_{a_d b_d}$, $N_{a_d b_d}$

Once a_{d_1}, b_{d_1} and a_{d_2}, b_{d_2} are identified from two tensile tests with different engineering strain rates $\dot{\varepsilon}_1$ and $\dot{\varepsilon}_2$, the parameters K_{a_d}, N_{a_d}, $K_{a_d b_d}$, $N_{a_d b_d}$ can also be identified.

From (29a) it is possible to obtain

$$-K_{a_d}\dot{\varepsilon}_1 + N_{a_d} = a_{d_1}$$

and

$$-\left[-K_{a_d}\dot{\varepsilon}_2 + N_{a_d} = a_{d_2}\right]$$

Hence, combining these equations it is possible to obtain

$$K_{a_d}\left(\dot{\varepsilon}_2 - \dot{\varepsilon}_1\right) = a_{d_1} - a_{d_2} \Rightarrow K_{a_d} = \frac{a_{d_1} - a_{d_2}}{\dot{\varepsilon}_2 - \dot{\varepsilon}_1} \tag{34}$$

The parameter N_{a_d} can be obtained from the following equation

$$N_{a_d} = a_{d_1} + K_{a_d}\dot{\varepsilon}_1 \tag{35}$$

While from (29b) we have

$$\ln(K_{a_d b_d}) + N_{a_d b_d}\ln(\dot{\varepsilon}_1) = \ln(a_{d_1} b_{d_1})$$

and

$$-\left[\ln(K_{a_d b_d}) + N_{a_d b_d}\ln(\dot{\varepsilon}_2) = \ln(a_{d_2} b_{d_2})\right]$$

which combined give $N_{a_d b_d}$

$$N_{a_d b_d}\left[\ln(\dot{\varepsilon}_1) - \ln(\dot{\varepsilon}_2)\right] = \left[\ln(a_{d_1} b_{d_1}) - \ln(a_{d_2} b_{d_2})\right] \Rightarrow N_{a_d b_d} = \frac{\left[\ln(a_{d_1} b_{d_1}) - \ln(a_{d_2} b_{d_2})\right]}{\left[\ln(\dot{\varepsilon}_1) - \ln(\dot{\varepsilon}_2)\right]} \tag{36}$$

The parameter $K_{a_d b_d}$ can be obtained from the following equation

$$K_{a_d b_d} = \frac{a_1}{(\dot{\varepsilon}_1)^{N_{a_d b_d}}} \tag{37}$$

4.4 Identification of K_d

The parameter K_d can be identified from the strain *vs* damage curves obtained in a tensile test with constant strain rates $\dot{\varepsilon}_1$ and $\dot{\varepsilon}_2$. The value η

$$\eta = \frac{K_d}{b}$$

can be obtained from both experimental damage curves, considering an avarage value. Hence, we have

$$K_d = \frac{b_1\eta_1 + b_2\eta_2}{2} \quad \text{and} \quad \eta_i = \frac{K_d}{b_i} \tag{38}$$

4.5 Determination of material parameters for magnesium alloy AZ31 at 375 ºC with initial grain size d = 17μm

The experimental damage curves shown in Fig 16 have been obtained for the investigated strain rates $\dot{\varepsilon}_1 = 0,0003$ (1/sec) and $\dot{\varepsilon}_2 = 0,01$ (1/sec).

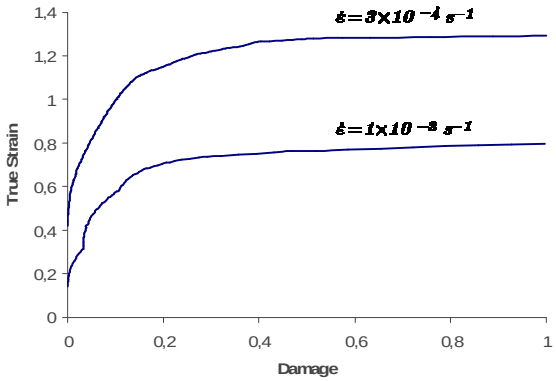

Figure 16: Damage curves for $\dot{\varepsilon}_1 = 0,0003$ (1/sec) and $\dot{\varepsilon}_2 = 0,01$ (1/sec).

For $\dot{\varepsilon}_1 = 0,0003$ (1/sec) the model curve which fits the experimental corrected damage curve gives $\eta_1 = 0,067$, $a_{d_1} = 1,12$ and $a_{d_1} b_{d_1} = 13,44$

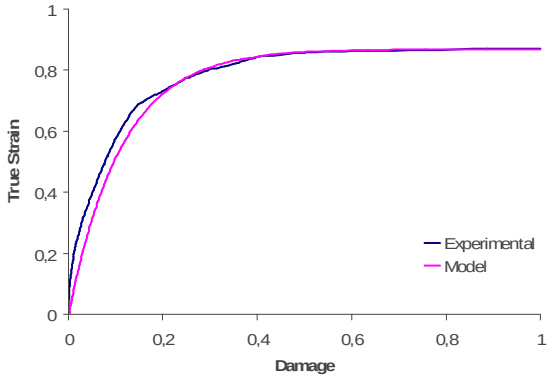

Figure 17: Corrected damage curve. Model and experiment. $\dot{\varepsilon}_1 = 0,003$ (1/sec).

While for $\dot{\varepsilon}_2 = 0,01$ (1/sec) the model curve gives $\eta_2 = 0,12$, $a_{d_2} = 0,72$ and $a_{d_2} b_{d_2} = 7,92$

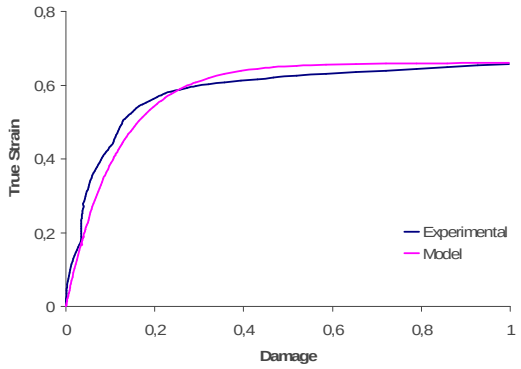

Figure 18: Corrected damage curve. Model and experiment. $\dot{\varepsilon}_2 = 0,01$ (1/sec).

Thus, from (34), (35), (36) and (37) it is possible to obtain $N_{a_d} = 1,16$; $K_{a_d} = -43,29$; $N_{a_d b_d} = -0,13$; $K_{a_d b_d} = 4,28$ while relation (38) gives $K_d = 8,71$. Hence, the following coefficients were identified for the examined magnesium alloy while the related model curves shown in figure 19 have been obtained.

$$a_1 = 16,20 \text{ MPa} \; ; \; a_1 b_1 = 1130,5 \text{ MPa} \; ; \; a_2 = 38,99 \text{ MPa} \; ; \; a_2 b_2 = 5068,7 \text{ MPa} \; ;$$
$$N_a = 68,92 \; ; \; K_a = 6,50 \; MPa \; ; \; N_{ab} = 10236 \; ; \; K_{ab} = 1122,1 \; MPa \; ; \; K_d = 8,71$$
$$a_{d_1} = 1,15 \; ; \; a_{d_1} b_{d_1} = 12,65 \; ; \; a_{d_2} = 0,73 \; ; \; a_{d_2} b_{d_2} = 7,92 \; ;$$
$$N_{a_d} = 1,16 \; ; \; K_{a_d} = -43,29 \; ; \; N_{a_d b_d} = -0,13 \; ; \; K_{a_d b_d} = 4,28$$

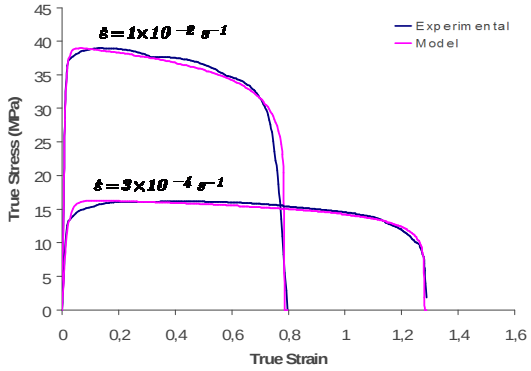

Figure 19: Stress-strain curve for $\dot{\varepsilon}_1 = 0,0003$ (1/sec) and $\dot{\varepsilon}_2 = 0,01$ (1/sec) for a magnesium alloy AZ31B-F at 375 °C.

5 Proposed model

From section (3) and (4) the model equations can be summarized as follows:

$$\sigma_t = (1 - D)\; a\; [1 - \exp(-b\varepsilon_t)] \quad \text{with} \quad 0 \leqslant D \leqslant 1$$

Where

$$D = \begin{cases} 0, \text{ if AUX} > 1 \\ -\left[\dfrac{1}{b_d}\right] \ln(AUX) \text{ , if } 0 < AUX < 1 \quad \text{with} \quad AUX = 1 - \left(\dfrac{\varepsilon_t \text{ - } \mathrm{K_d/b}}{a_d}\right) \\ 1, \text{ if } AUX < 0 \end{cases}$$

and

$$\ln(\mathrm{e^a} \text{ - } 1) = K_a \ln(\dot{\varepsilon}) + N_a, \quad \ln\left(\mathrm{e^{ab}} \text{ - } 1\right) = K_{ab} \ln(\dot{\varepsilon}) + N_{ab} \text{ , } \quad \mathrm{AUX} = 1 \text{ - } \left(\tfrac{\varepsilon_t \text{ - } [\mathrm{K_d}/b]}{a_d}\right) \text{ ,}$$
$$a_d = -K_{a_d}(\dot{\varepsilon}) + N_{a_d}, \quad \mathrm{a_d b_d} = K_{a_d b_d}[\dot{\varepsilon}]^{-N_{a_d b_d}}$$

Using the coefficient previously identified, it is now possible to predict the mechanical behavior of the same magnesium alloy deformed at the same conditions but at a different value of engineering strain rate.

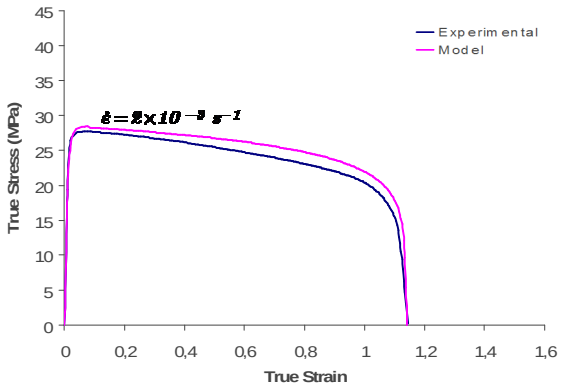

Figure 20: Stress-strain curve for $\dot{\varepsilon} = 0,002$ (1/sec) for a magnesium alloy AZ31 at 375 °C ($a_0 = a_0 b_0 = 0$).

Fig 20 shows the good approximation of the experimental true stress vs true strain curve achieved by the model curve for an intermediate strain rate $\dot{\varepsilon} = 0,002$ (1/sec).

Further good results have been observed applying the model to the step test experimental data taken from Del Valle [12] and referred to the same material tested in the previous tensile tests.

As shown in figure 21b, unrealistic previsions of the superplastic behavior can be observed for the lowest strain rates as $\dot{\varepsilon} = 0,000075$ (1/sec) $\dot{\varepsilon} = 0,00002$ (1/sec). Such limitation can be circumvented by taking the parameters a_o and b_o different from zero. When nonzero values are assumed for a_0 and b_0, good fitting curves can be obtained even for low values of strain rate as it can be seen in figure 22a-b.

The hypothesis of nonzero values for a_0 and b_0 suggest, as reported by literature, an evidence of some form of threshold stress for superplastic flow since dislocation activity is not normally observed at lower strain rates. Nevertheless, when tensile tests are carried out at such strain rates, grain grow and an associated hardening effect are usually observed. According to Del Valle [12], grain growth during tensile test at $\dot{\varepsilon} = 0,00005$ (1/sec) is reported. In this case model curve differs from experimental curve as show in fig 20.

The model seems then able to predict the experimental results obtained when grain growth is inhibited (step test), while it leads to results that disagree from experimetal ones when grain growth takes place.

This aspect suggests a possible application of the model to evaluate the hardening associated with grain growth during low strain rate tests.

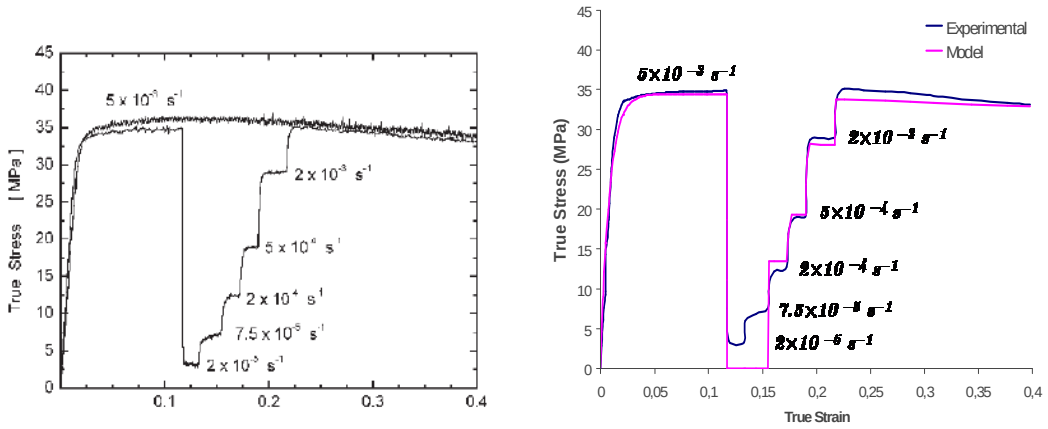

(a) (b)

Figure 21: Step Test curve from Del Valle [10] and model for a magnesium alloy AZ31 at 375 ºC ($a_0 = a_0 b_0 = 0$).

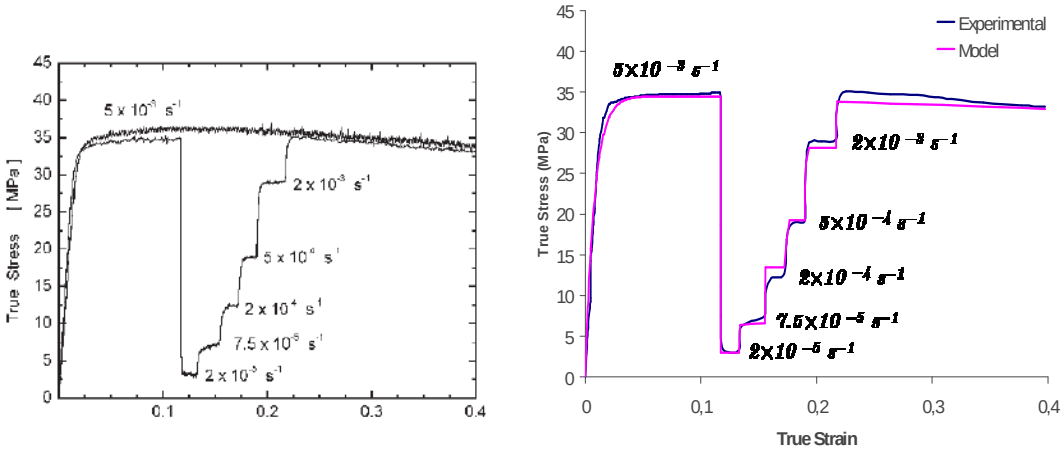

(a) (b)

Figure 22: Step Test curve from Del Valle [10] and model curve for a magnesium alloy AZ31 at 375 ºC ($a_0 = 3$, $a_0 b_0 = 135$).

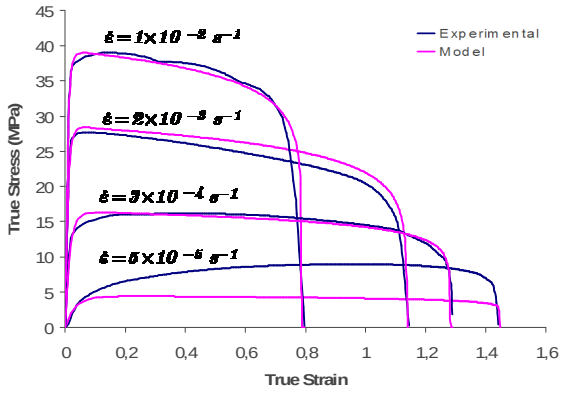

Figure 23: Stress-strain curve for different engineering strain rates for a magnesium alloy AZ31 at 375 ºC ($a_0 = 3$, $a_0 b_0 = 135$).

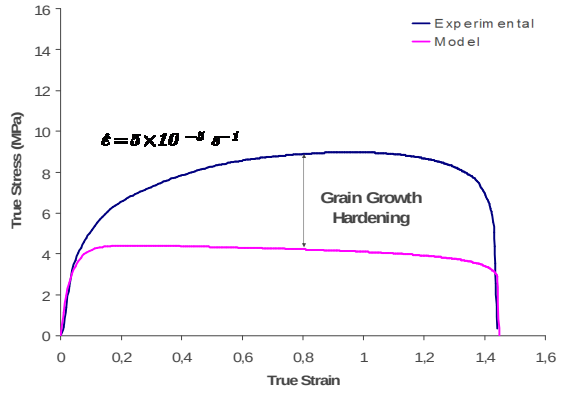

Figure 24: Evaluation of grain growth hardening from model and experimental curve for a magnesium alloy AZ31 at 375 ºC.

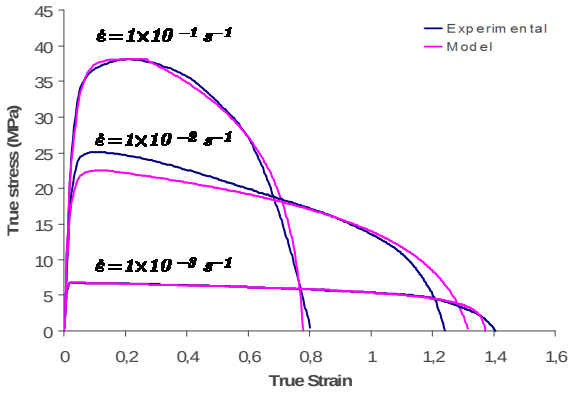

Figure 25: Stress-strain curve for different engineering strain rates for a magnesium alloy AZ31 at 500 °C.

Good predictions have also been obtained considering the experimental results from Xin Wu [3], referred to tensile tests carried out at 500 °C on AZ31 magnesium alloy with initial grain size d =300μm. In this case, the following coefficients were identified:

$$a_1 = 6,85 \text{ MPa} \; ; \; a_1 b_1 = 1370,0 \text{ MPa} \; ; \; a_2 = 38,12 \text{ MPa} \; ; \; a_2 b_2 = 1486,6 \text{ MPa} \; ;$$
$$N_a = 53,75 \; ; \; K_a = 6,79 \; MPa \; ; \; N_{ab} = 1545,0 \; ; \; K_{ab} = 25,33 \; MPa \; ; \; K_d = 9,16$$
$$a_{d_1} = 1,3 \; ; \; a_{d_1} b_{d_1} = 8,11 \; ; \; a_{d_2} = 0,53 \; ; \; a_{d_2} b_{d_2} = 1,89 \; ;$$
$$N_{a_d} = 1,30 \; ; \; K_{a_d} = -7,77 \; ; \; N_{a_d b_d} = -0,31 \; ; \; K_{a_d b_d} = 0,91$$

Figure 22 presents the experimental curves and model prevision for three different strain rates.

6 One-dimensional problem with compression

The previous model is only adequate for monotone problems ($\dot{\varepsilon} \geqslant 0$). In order to build a more general model, the first step is to include the possibility of non-monotone loadings. In this case, a new additional auxiliary variable must be considered – the cumulated plastic strain p, classically defined as follows:

$$p(t) = \int_{t=0}^{t} |\dot{\varepsilon}_t(\xi)| \; d\xi \Rightarrow \dot{p}(t) = |\dot{\varepsilon}_t(t)| \tag{39}$$

From definition (39) it is easy to verify that $p(t) = \varepsilon(t)$, in a tensile test with $\dot{\varepsilon}(t) \geqslant 0$. It is also possible to obtain that $p(t) = -\varepsilon(t)$ in a tensile test with $\dot{\varepsilon}(t) \leqslant 0$. Hence, the following model equations are proposed (the material parameters are the same from the model proposed in the last sections, and also their experimental identification)

$\sigma_t = (1-D)X$

Where

$\dot{X} = ab\dot{\varepsilon}_t - bX\dot{p}$

$p(t) = \int_{t=0}^{t} |\dot{\varepsilon}_t(\xi)| \; d\xi \Rightarrow \dot{p}(t) = |\dot{\varepsilon}_t(t)|$

$$D = \begin{cases} 0, \text{ if } AUX > 1 \\ -\left[\frac{1}{b_d}\right] \ln(AUX) \text{ , if } 0 < AUX < 1 \text{ with AUX = 1 - } \left(\frac{p - K_d/b}{a_d}\right) \\ 1, \text{ if } AUX < 0 \end{cases}$$

and

$\ln(\mathrm{e^a} - 1) = K_a \ln(\exp(p)\ \dot{p}) + N_a, \quad \ln\left(\mathrm{e^{ab}} - 1\right) = K_{ab} \ln(\exp(p)\ \dot{p}) + N_{ab},$

$\mathrm{AUX} = 1 - \left(\frac{\varepsilon_t - [\mathrm{K_d}/b]}{a_d}\right) , \quad a_d = -K_{a_d}(\exp(p)\ \dot{p}) + N_{a_d}, \quad \mathrm{a_d b_d} = K_{a_d b_d}[\exp(p)\ \dot{p}]^{-N_{a_d b_d}}$

To better understand the role of the variable X in the present model, it is interesting to verify the mechanical behavior described by the above presented equations in the case of monotone loading histories.

From the definition of the cumulated plastic strain p we have:

$$\dot{X} = ab\dot{\varepsilon}_t - bX\,|\dot{\varepsilon}_t| \tag{40}$$

In a tensile test with $\dot{\varepsilon}(t) \geqslant 0$ it is possible to obtain:

$$\dot{X} = ab\dot{\varepsilon}_t - bX\dot{\varepsilon}_t \Rightarrow \frac{dX}{d\varepsilon_t} = b\,(a - X) \tag{41}$$

Hence, for an initial condition $(X_\mathrm{i}, \varepsilon_i) \Rightarrow X = a + [(X_i - a)\ \exp(-b(\varepsilon_t - \varepsilon_i))]$, the true stress is given by the following expression:

$$\sigma_t = (1-D)\ \left(\ a + [(X_i - a)\ \exp(-b(\varepsilon_t - \varepsilon_i))]\ \right) \tag{42}$$

If $X_\mathrm{i} = 0$ and $\varepsilon_i = 0$, the above equation is the same proposed for the monotone case in section 4 (equation 23).

In a tensile test with $\dot{\varepsilon}(t) \leqslant 0$ it is also possible to obtain:

$$\dot{X} = ab\dot{\varepsilon}_t + bX\dot{\varepsilon}_t \Rightarrow \frac{dX}{d\varepsilon_t} = b(a + X) \tag{43}$$

Hence, for an initial condition $(X_\mathrm{i}, \varepsilon_i) \Rightarrow X = -a + [(X_i + a)\ \exp(b(\varepsilon_t - \varepsilon_i))]$, the true stress is given by the following expression:

$$\sigma_t = (1-D)\ \left(\ -a + [(X_i + a)\ \exp(b(\varepsilon_t - \varepsilon_i))]\ \right) \tag{44}$$

Figure 24 shows the stress-strain curve for a magnesium alloy AZ31B-F at 375 ºC considering the loading history presented at figure 26

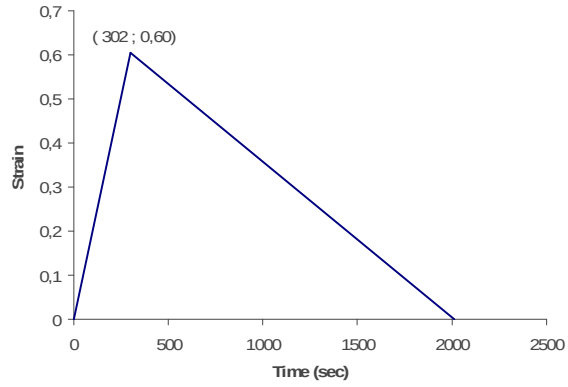

Figure 26: Non-monotone loading history.

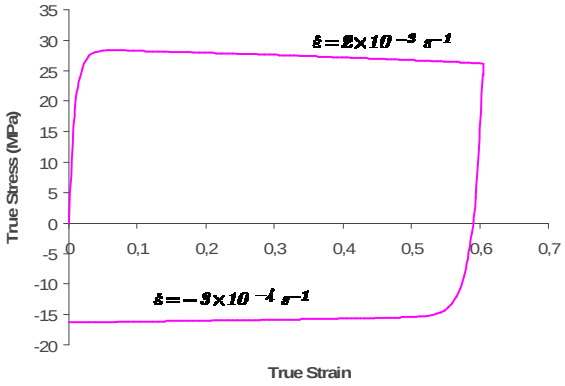

Figure 27: Stress-strain curve for the non-monotone loading history presented at figure 26, for a magnesium alloy AZ31B-F at 375 ºC.

7 Concluding remarks

The one-dimensional phenomenological damage model proposed on this paper is able to perform a mathematically correct and physically realistic description of plastic deformations, strain hardening, strain softening, strain rate sensitivity and damage observed in tensile tests performed at different strain rates and temperatures.

The identification of parameters that appear in the theory is discussed in detail and examples concerning the modeling of tensile tests of a magnesium alloy at different strain rates and temperatures

are presented and analyzed. It is necessary to perform only two tensile tests at different strain rates in order to identify the parameters that appear in the theory. The results obtained show a very good agreement between experimental results and model prevision for different strain rates.

Finally, it is important to observe that it is necessary to adapt such model to account for compression loading, what can be done through the introduction of a new auxiliary variable related to the cumulated plastic strain.

It is also necessary an adequate thermo mechanical framework in order to extend the proposed model to a tri-dimensional context, which is essential since one of the main practical motivation to study such alloys is the superplastic forming (SPF) of sheet metals. In a tri-dimensional context, the adequate choice of the measure of strain and of the objective time derivative is essential to build a physically realistic and mathematically correct model [14].

References

[1] Khaleel, M.A., Zbib, H.M. & Nyberg, E.A., Constitutive modeling of deformation and damage in superplastic materials. *International Journal of Plasticity*, **17**, pp. 277–296, 2001.

[2] Kim, W.J., Chung, S.W., Chung, C.S. & Kum, D., Superplasticity in thin magnesium alloy sheets and deformation mechanism maps for magnesium alloys at elevated temperatures. *Acta Mater*, **49**, pp. 3337–3345, 2001.

[3] Xin, W. & Yi, L., Superplasticity of coarse-grained magnesium alloy. *Scripta Materialia*, **46**, pp. 269–274, 2002.

[4] Tan, J.C. & Tan, M.J., Superplasticity in a rolled Mg-3Al-1Zn alloy by two-stage deformation method. *Scripta Materialia*, **47**, pp. 101–106, 2002.

[5] Somekawa, H., Hosokawa, H., Watanabe, H. & Higashi, K., Diffusion bonding in superplastic magnesium alloys. *Materials Science and Engineering*, **A339**, pp. 328–333, 2003.

[6] Lin, H.K., Huang, J.C. & Langdon, T.G., Relationship between texture and low temperature superplasticity in an extruded AZ31 Mg alloy processed by ECAP. *Materials Science and Engineering*, **A402**, pp. 250–257, 2005.

[7] Takuda, H., T., M., Kinoshita, T. & Shirakawa, N., Modelling of formula for flow stress of a magnesium alloy AZ31 sheet at elevated temperatures. *Journal of Materials Processing Technology*, **164-165**, pp. 1258–1262, 2005.

[8] Yin, D.L., Zhang, K.F. & Wang, G.F., Microstructure evolution and fracture behavior in superplastic deformation of hot-holled AZ31 Mg alloy sheet. *Materials Science Forum*, **475-479**, pp. 2923–2926, 2005.

[9] Yin, D.L., Zhang, K.F., Wang, G.F. & Han, W.B., Superplasticity and cavitation in AZ31 Mg alloy at elevated temperatures. *Materials Letters*, **59**, pp. 1714–1718, 2005.

[10] Lee, B.H., Shin, K.S. & Lee, C.S., High temperature behavior of AZ31 Mg alloy. *Materials Science Forum*, **475-479**, pp. 2927–2950, 2005.

[11] ASTM Standard E 2448-05, *Standard Test Method for Determining the Superplastic Properties of Metallic Sheet Materials.*

[12] Del Valle, J.A., Pérez-Prado, M.T. & Ruano, O.A., Deformation mechanisms responsible for the high ductility in a Mg AZ31 alloy analyzed by electron backscattered diffraction. *Metallurgical And Materials Transactions A*, **Volume 36A**, pp. 1427–1438, 2005.

[13] Chandra, N., Constitutive behavior of superplastic materials. *International Journal of Non-Linear*

Mechanics, **37**, pp. 461–484., 2002.

[14] Costa-Mattos, H., A thermodynamically consistent constitutive theory for fluids. *International Journal of Non-linear Mechanics*, **33(1)**, pp. 97–110, 1998.

Mechanics of Solids in Brazil 2009, H.S. da Costa Mattos & Marcílio Alves (Editors)
Brazilian Society of Mechanical Sciences and Engineering, ISBN 978-85-85769-43-7